

FLORIDA INTERNATIONAL UNIVERSITY

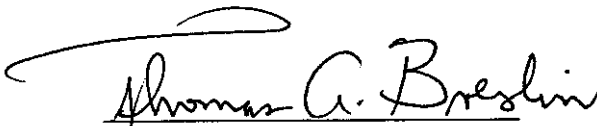
GRANTS FOR AVIATION RESEARCH
Cooperative Agreement Proposal

PHASE II
FINAL REPORT
GRANT 00-G-0026

PANTHERSKIN™ PROJECT



Dr. Milton J. Torres
Research Scientist
Industrial Engineering Department
Principal Investigator



Dr. Thomas A. Breslin
Vice President Research
Florida International University



Dr. Kuang-Hsi Wu
Professor
Mechanical Engineering Department
Co-Principal Investigator

FINAL REPORT

The PANTHERSKIN™ project as requested in the RFP could not be complete without the additional investigations that will be discussed that follows below in this report. The report will have the following sections: *Areas of Investigation; Results of the Investigation; Total properties of a PANTHERSKIN™ application for existing or new aircraft; Conclusions; Recommendations;*

The latest and newest investigations will be discussed initially and then we will briefly list the total properties of PANTHERSKIN™ as a new millennium insulant with more properties than just the insulation factor. The conclusion of the investigation of this grant will be discussed as follows:

- A. MATERIAL PROPERTIES (STRENGTH)
- B. FIRE RESISTANCE
- C. ACOUSTICAL PROPERTIES
- D. FINITE ELEMENT STUDY W/BONDED STRINGERS

AREAS OF INVESTIGATION

A. MATERIAL PROPERTIES (STRENGTH)

In the formation of the Pantherskin foam it has to be understood the basic process of changing phase from a liquid into a foam. Initially the foam is made by a chemical reaction of a polyol (multiple functionality of large alcohol polymer family) and a polyisocyanate. The precise mix of a continuous stream calculated to form a foam that contains the lowest k factors and thermal conductivity and the ability to strengthen the fuselage structure. The fluids are processed though a proportioning machine that delivers the foam stoichiometrically correct at a hand held spray valve. The spray is evenly spread on the inside wall of the fuselage and the layer is first wet smoothly and evenly. In the expansion phase a formation of closed cell bubbles grows approximately 30 times it normal volume. The smoother the spray application the smoother the rising surface. A layer is formed to a desired thickness sealing and forming a protective layer of foam. While the foam is rigid it is flexible enough to yield to pressures without cracking. It is the tensile strength of this foam that reduces the strains applied to the fuselage allowing movement of the skin without fracture or skin cracks of any kind.

This study involved the molding of several bone shaped test specimens for insertion into an Instron machine to discover its tensile strength by elongation until the point of fracture. When the foam continues to expand until the chemical reaction is at completion it was known to have a curing time. Various conditions such as formation temperatures, ambient pressures and temperatures would continue the reaction until the

reaction would yield a 100% cure. The initial cure would permit the usage of the foam with a reasonable strength up until approximately 26 weeks where a full cure strength would be reached. In order to know what strengths would be achieved the samples had to be formed of various densities and conditions and tested periodically from 1 week at intervals of a week apart up to approximately 12 weeks and then at intervals greater than 2 weeks apart until 26 weeks. This required various batches of chemical and thousands of samples to stretch out the testing until full strength is achieved. The results of the testing of the bone shaped samples are depicted in the graph in Appendix A. At the same time various densities of samples were formed and investigation of how the strength would increase as the density increased.

B. FIRE RESISTANCE

Recently the FAA has established a new fire resistance standard and it was mandated that any accepted material would in fact be able to pass this new criteria. The oil burner system would be directed against a curved panel and the requirement was to be able to withstand the fire generated by the high BTU generated oil burner for a total of 5 minutes. One minute for the skin and then four minutes for the insulation. An old formulation established that the proper flame retardant in lieu of a newer flame retardant that was cheaper but did not pass the test. The older flame retardant proved to be the chemical for usage in this test. Two samples were sent to the William J. Hughes Technical Center for the test. One was an L1011 skin covered with curlon and sprayed with 3.5 inches of PANTHERSKIN™ and a second L1011 panel with only a 3.5 inch layer of PANTHERSKIN™. The results of these tests is listed in the Results section of this report.

C. ACOUSTICAL

We enlisted the cooperation of the Orcon Corporation to donate some of their Curlon for this test and the question came up on how the PANTHERSKIN™ would behave acoustically. Panels were prepared and shipped to Orcon in California for the acoustical tests. One panel was prepared with Curlon and the other with just the foam. The results are depicted in the Appendix C of this report.

D. FINITE ELEMENT STUDY W/BONDED STRINGERS

In the initial agreement to investigate using the FEM study a bonded stringer section. A complete study was performed and the entire study is included with this report and an initial finding is shown in the Appendix D for your perusal.

RESULTS OF THE INVESTIGATION

A. MATERIAL PROPERTIES (STRENGTH)

Thousands of bone shaped test pieces were made and only those that had no external cracks fissures or any kind of detail were accepted with any visible flaw being grounds for rejection of the sample. In many cases an unusual flaw was found after the testing was completed. These samples were not necessarily counted if any obvious flaws were visible and before long the justifiable and obvious were a much smaller propagation. In all cases the numbers were accepted if they were somewhere near the ball park. In Appendix A some very obvious correlations were happening. To whit; neither group was automatically accepted or rejected. When the final data was observed it was accepted unless it had a serious crack or deformation with respect to the samples it was accepted. The samples were generally accepted and plotted by temperature profile and some were interested in the stress under a completely different set of starting points. A collective series were sorted and graphed by age in weeks to see what difference there was between the strength and the formation temperature. The graph shows very little difference between the overall strength and the formation temperature. Upon inspection of the graph in the Appendix A it can be observed that the formation temperature has little effect on the overall strength. The significant difference was those specimens containing Kevlar showing that indicated the Kevlar based specimens were on the order of 4 times stronger than the specimens without Kevlar.

The theoretical plot of PANTHERSKIN™ stems from the original formulator, at Mobil Chemical, later at Albright Wilson as chief scientist, Dr James Anderson. His simple explanation was that the strength of the foam would go up as the square of the density. This is noted on the Density vs. Strength graph as the dark straight line call the theoretical slope. The actual density was plotted in red and we were limited to just six pounds per cubic foot density foam. While it is very possible to have much higher densities we focused on the 2 - 4 lb density as this would be the recommended densities for utilization in aircraft. Note that while we do not see a direct correlation to the theory it seems that the slope of the line approximates the actual values.

B. FIRE RESISTANCE

In studying the properties of PANTHERSKIN™ several different types of tests were made to insure that the foam would not add to the burning of an aircraft and offer some protection to the occupants of a survivable crash. Standardization took effect within the FAA and the organization settled on a 4 min requirement for burn through on a very high BTU output oil burner. In order to establish a positive burn through a decision to burn the PANTHERSKIN™ sprayed panel with and without the addition of Curlon to insure a successful burn. The curlon was totally covered by the foam and it proved to be even more successful than just the PANTHERSKIN™ alone. Photographs and times of the final burn on both cases are displayed in Appendix B. These are the actual times to burn through from the tests done at the William J. Hughes Technical Center in Atlantic City.

C. ACOUSTICAL PROPERTIES

The Orcon Corp not only gave us sample material for our tests, but they conducted acoustical test to see how PANTHERSKIN™ would react acoustically compared to Microlite. In comparison with the two samples sent it appears that both the samples with or without Curlon performed better than the Microlite by itself. This suggests that while the PANTHERSKIN™ is somewhat better acoustically than existing insulations but the Curlon improved in the attenuation of noise somewhat better than the foam alone.

D. FINITE ELEMENT STUDY W/BONDED STRINGERS

A finite element model for the fuselage panel section was constructed and subjected to a uniform pressure of 8.5 psi in addition to an edge load. The fuselage section was modeled as follows:

1. Fuselage panel without Foam.
2. Fuselage panel with a 1.5 inch foam layer.
3. Fuselage panel with a 2 inch foam layer.

The Von Mises stress at the most critical location was collected and the results are compared in the figure in Appendix D. As can be seen the maximum stress level decreased with the increasing foam thickness. This indicates that the foam has a mitigating effect on the stress levels in the fuselage section which have direct implication on the life of the fuselage section. Details on the finite element study will be in the attached Finite Element Analysis attached to this report.

TOTAL PROPERTIES OF A PANTHERSKIN™ APPLICATION FOR EXISTING OR NEW AIRCRAFT

The initial investigation of the PANTHERSKIN™ project has been conducted primarily in the laboratories of the Industrial Engineering department at Florida International University. However, some of the investigations have been extensively examined at places determined by the USN and the FAA and in the EF3 experiments in Hamburg, Germany for the A340. The FAA at Sandia knowing that Eddy Current testing would eventually have to detect cracks in skins coated a multiflawed panel w/several types of flaws. Their findings will be reported by the FAA in the final report issued by them. The investigation has consisted of the following areas of research.

1. Strain Measurements of Aircraft Skin.
2. Fire Resistance at High Temperatures.
3. Cyclic Stress Evaluations.
4. Corrosion Experiments on Aircraft Skin.

5. Corrosion Experiments on Carbon Steel
6. Chemical Resistance of PANTHERSKIN™.
7. Crack Propagation on A340 EF3
8. Cure Strength Study on A310 fuselage section
9. Explosion test on Aircraft Aluminum Box.
10. Burn profile study.
11. Finite Element Analysis (FEA) of converted FAA program for PANTHERSKIN™.
12. Curved Panel Testing at the William J. Hughes FAA Technical Center.

In every case and at every type of determination the results have indicated positive in every way for utilization in aircraft for the safety and life extension of pressurized aircraft. Reduction of strain and lowering of crack propagation, along with the control of corrosion and added protection of cabin inhabitants from fire.

CONCLUSIONS

In the final analysis both by inhouse and external testing finds the following properties to be true. The last FEA correlates to all the other information from this study indicating a positive correlation to a reduction of strain on the fuselage. The aging aircraft can have the useful life extended for not less than two and up to five times by the addition of PANTHERSKIN™ by spraying a 2 - 3.5 inch thickness inside the fuselage. Along with this property we have gained Flame resistance from PANTHERSKIN™ and strengthening of the fuselage in case of survivable aircraft accidents. The increased structural integrity while adding an insulation with superior K factors and protection against flame intrusion of these same accidents. These properties make PANTHERSKIN™ an economically efficient addition of a new insulation for the mandate of replacing insulation.

The individual philosophy of airlines is to avail the public of newer and safer aircraft. However, the newest aircraft is immediately subjected to corrosion problems and an adjustment to a flame resistant insulation must also be made. It has been stated by Vice President of Delta Airlines (Ray Valika), at the Aging Aircraft Conference at Williamsburg VA that the philosophy of Delta is to rid themselves of all old airplanes and replace them with new airplanes. This philosophy is shared by most airline executives and with that philosophy it will mean disaster in the air as they are not addressing aging aircraft problems. Aircraft manufacturers will not endorse any life extension system on aircraft as that will mean less aircraft to manufacture. The FAA then must posture itself on the side of safety or will have to accept violent catastrophies such as the Aloha incident as being the price of the risk passengers and crews will have to take to continue as we have in the past. This philosophy is contrary to the stated FAA policy and to allow the executives of airlines to maintain this strategy would be to let the governed tell the government that safety is not a concern. If the FAA does not enact procedures to apply safety measures to insure the passenger and crew the safety they deserve would mean that the FAA is shirking its duty to the people of the country.

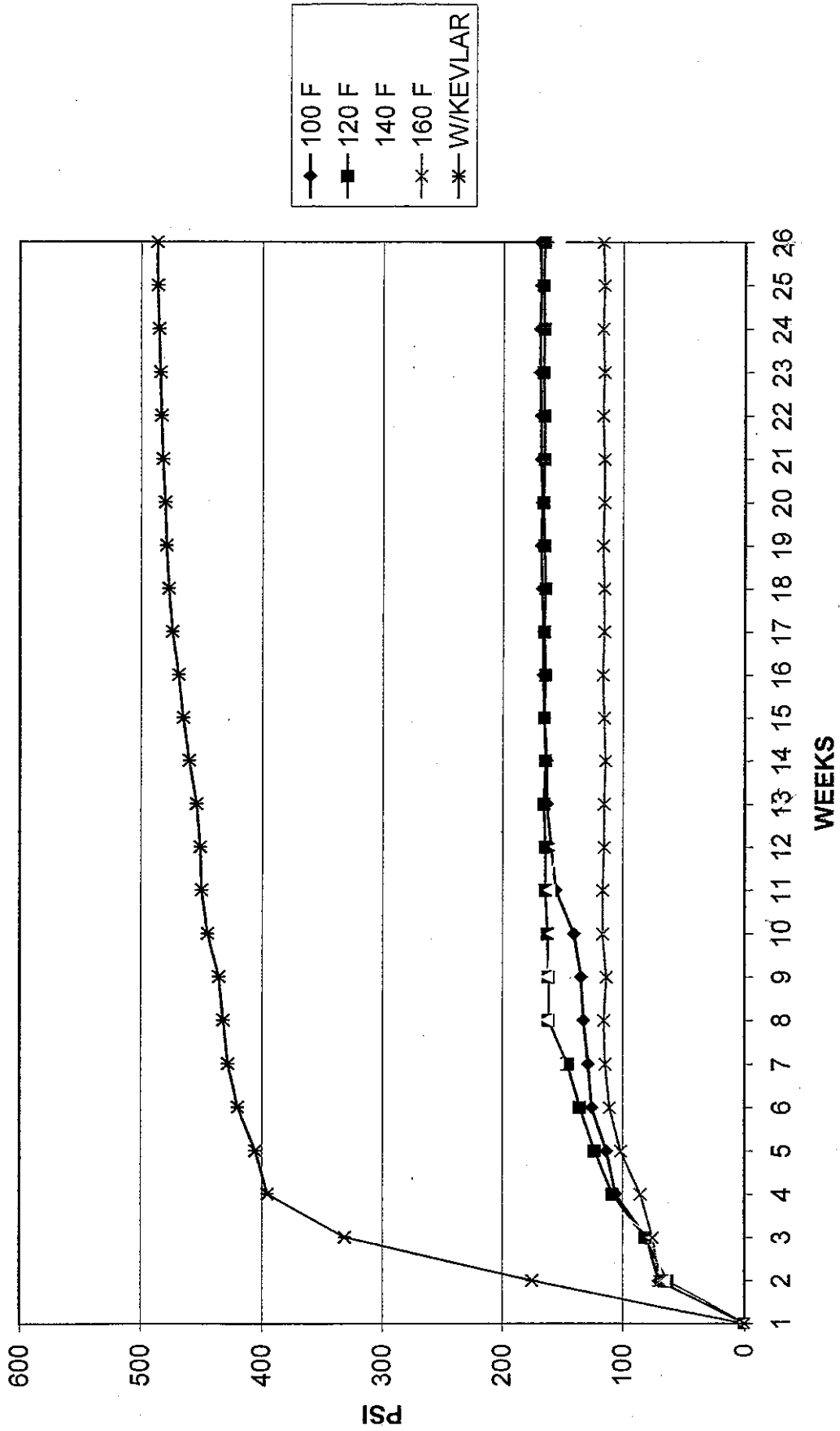
RECOMMENDATIONS

PANTHERSKIN™ has been found to have a great benefit to Aging Aircraft but can be tested further. Although bomb blast attenuation appears possible it has not been proven.

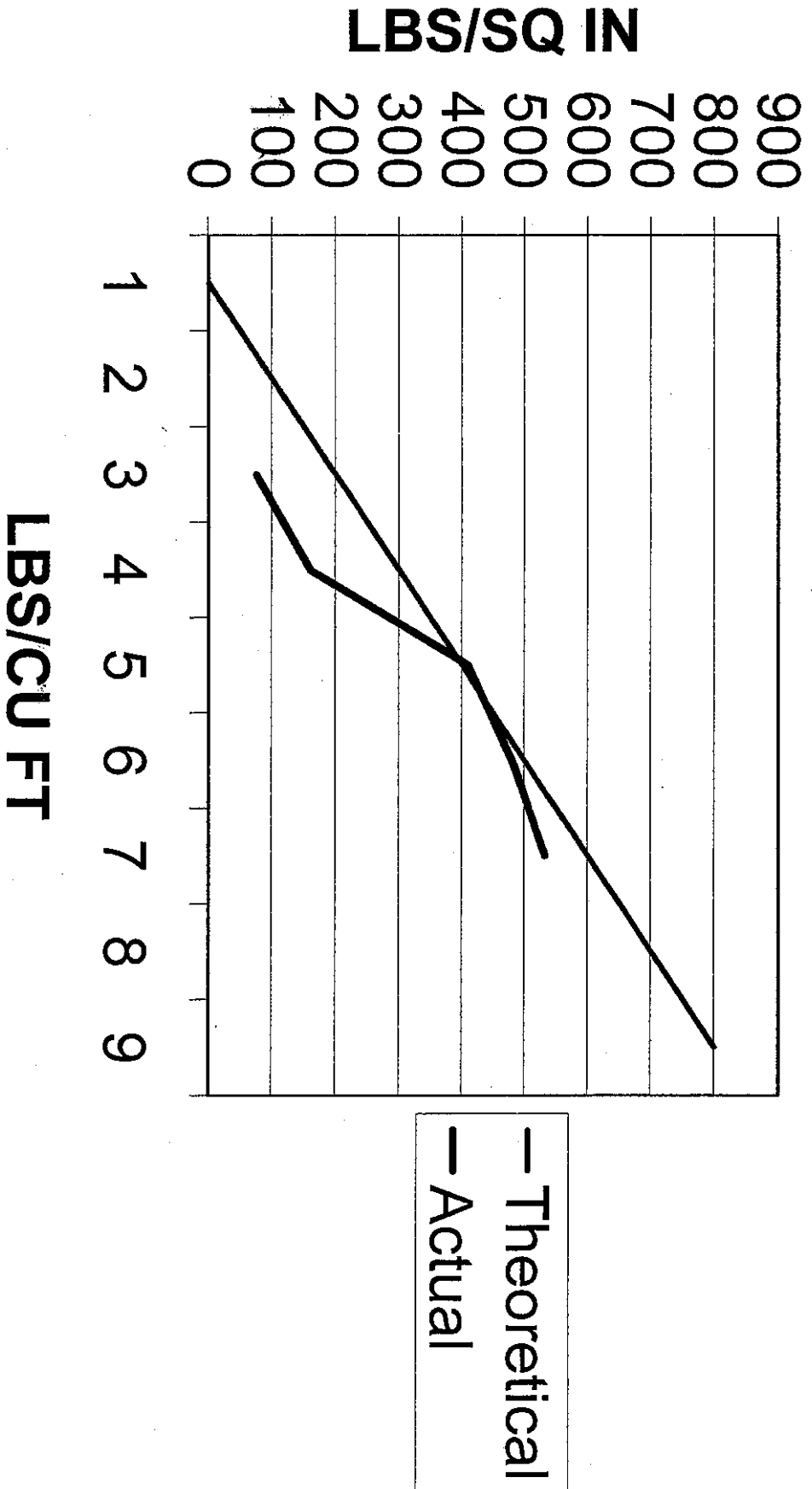
- (1). A Kevlar reinforced layer of PANTHERSKIN™ should be tested on a retired airframe to prove how effective this could be to reducing fear of terrorist bombings. Perhaps an area in the lower section should be designed as a blowout area with the remainder of the aircraft foamed-in could result in the elimination of concern for terrorists killing innocent people.
- (2) No airborne tests have confirmed the corrosion benefit of the foam. Therefore, it is recommended that efforts be made to find an aircraft having severe corrosion problems and that this airframe be tested by spraying a layer of foam and flying the aircraft in normal everyday flights to ascertain that the corrosion has been arrested.
- (3) The FAA has been very positive to accept thermal imaging or eddy current type inspections of aircraft to detect cracks. The old inspector with a flashlight checking for micro cracks or very large cracks is unable to detect many of the more subtle cracks. Case in point this was and to a large extent still is the methodology for crack detection. This procedure was very much in practice when the Aloha incident had the double whammy of crack formation and corrosion and still was not detected until after the incident. One of the old timers objections to coating an aircraft with foam is the inability to see the cracks because they were covered by the foam. Therefore, once eddy current is employed at major inspections this objection will no longer be valid. Old methods must be rejected and newer methods should be employed at all inspections. The time for PANTHERSKIN™ would be now along with these changes in inspection procedures.

Appendices

Material Properties Tensile Strength

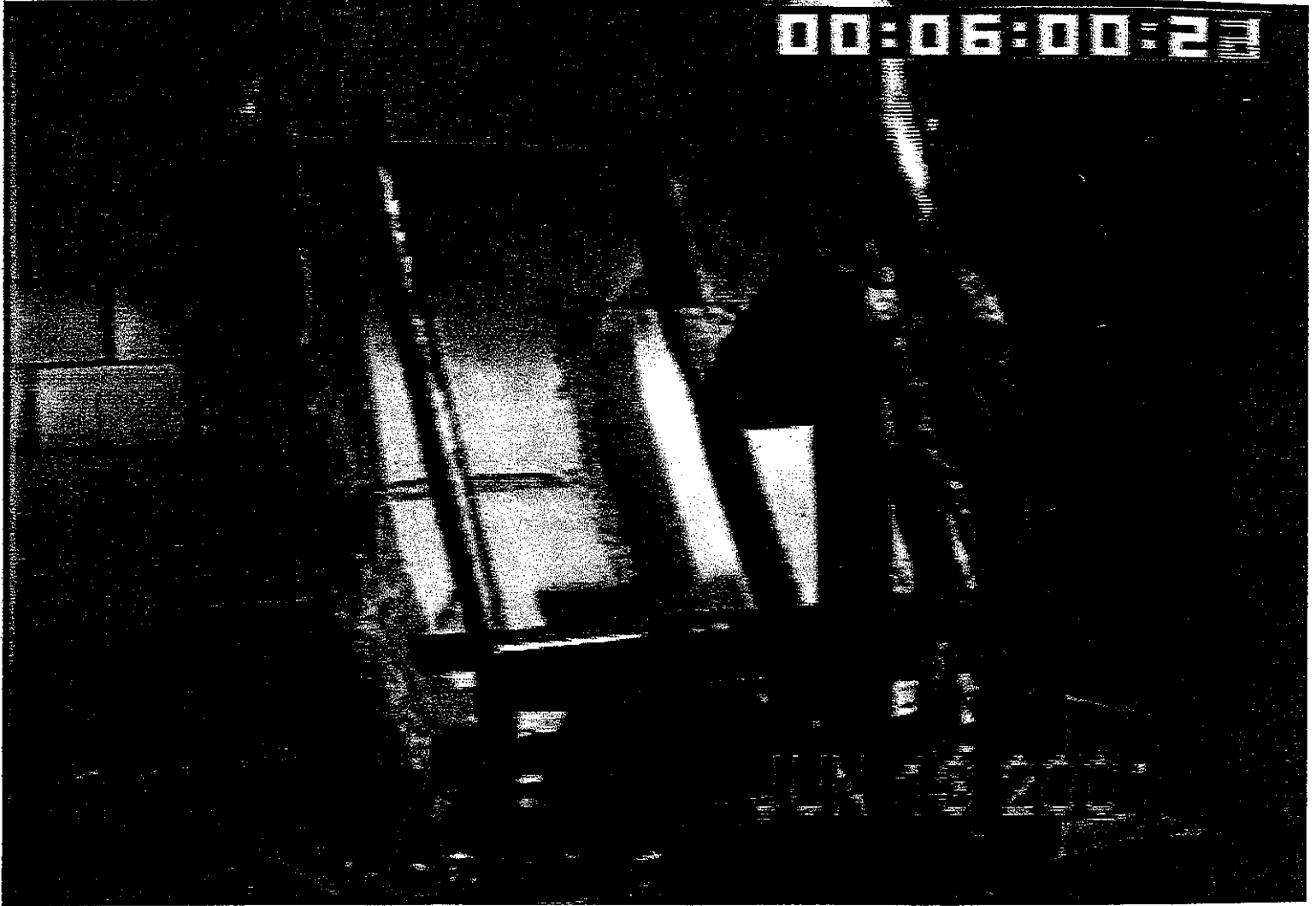


DENSITY VS. STRENGTH





PANTHERSKIN W/CURLON burnthrough

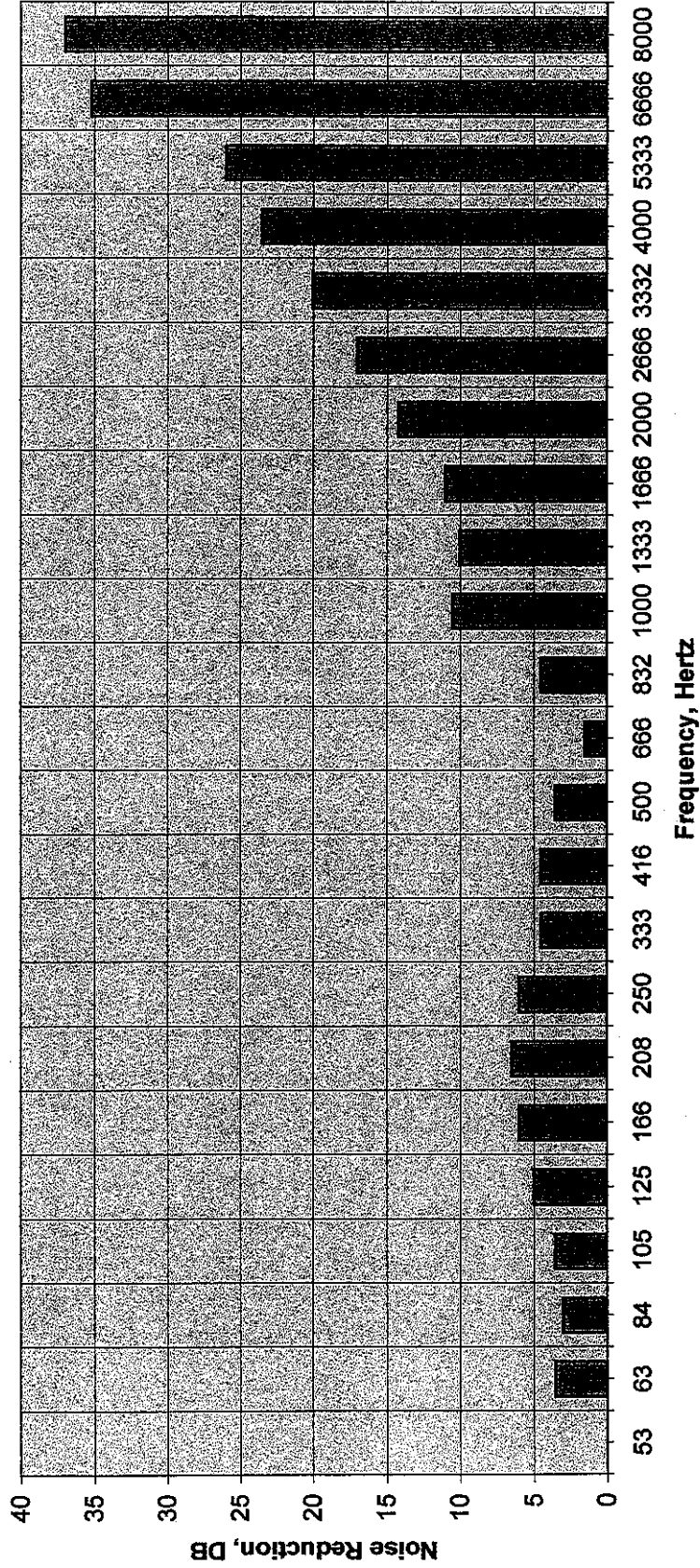


Only PANTHERSKIN Burnthrough

REVERBERATION CHAMBER MICROPHONE
ANECHOIC CHAMBER MICROPHONE
DATA NORMALIZED TO EMPTY TEST SPECIMEN FRAME

ORCON CORPORATION

Three 1 Inch Thick Layers Of 0.42 Lb/ft³ Microlite



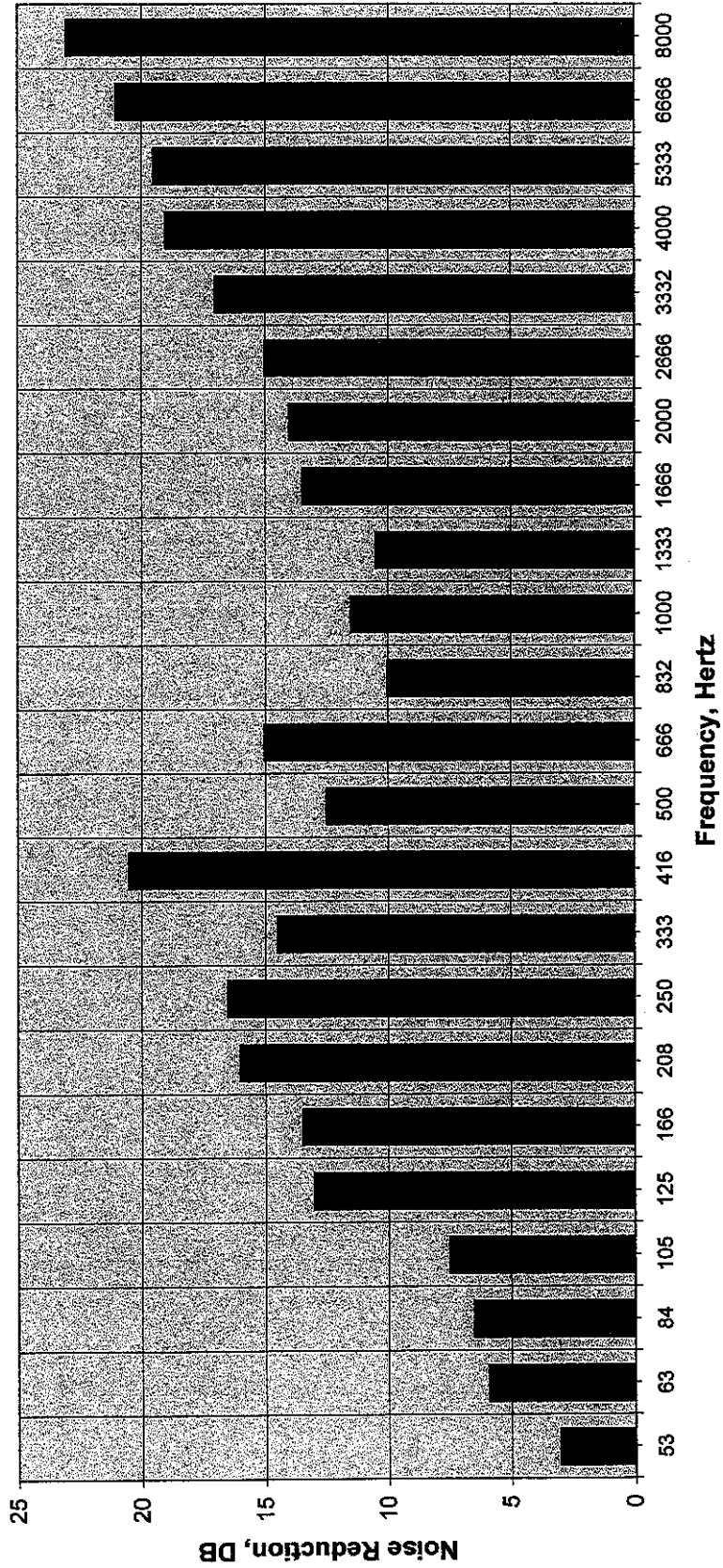
REVERBERATION CHAMBER MICROPHONE

ANECHOIC CHAMBER MICROPHONE

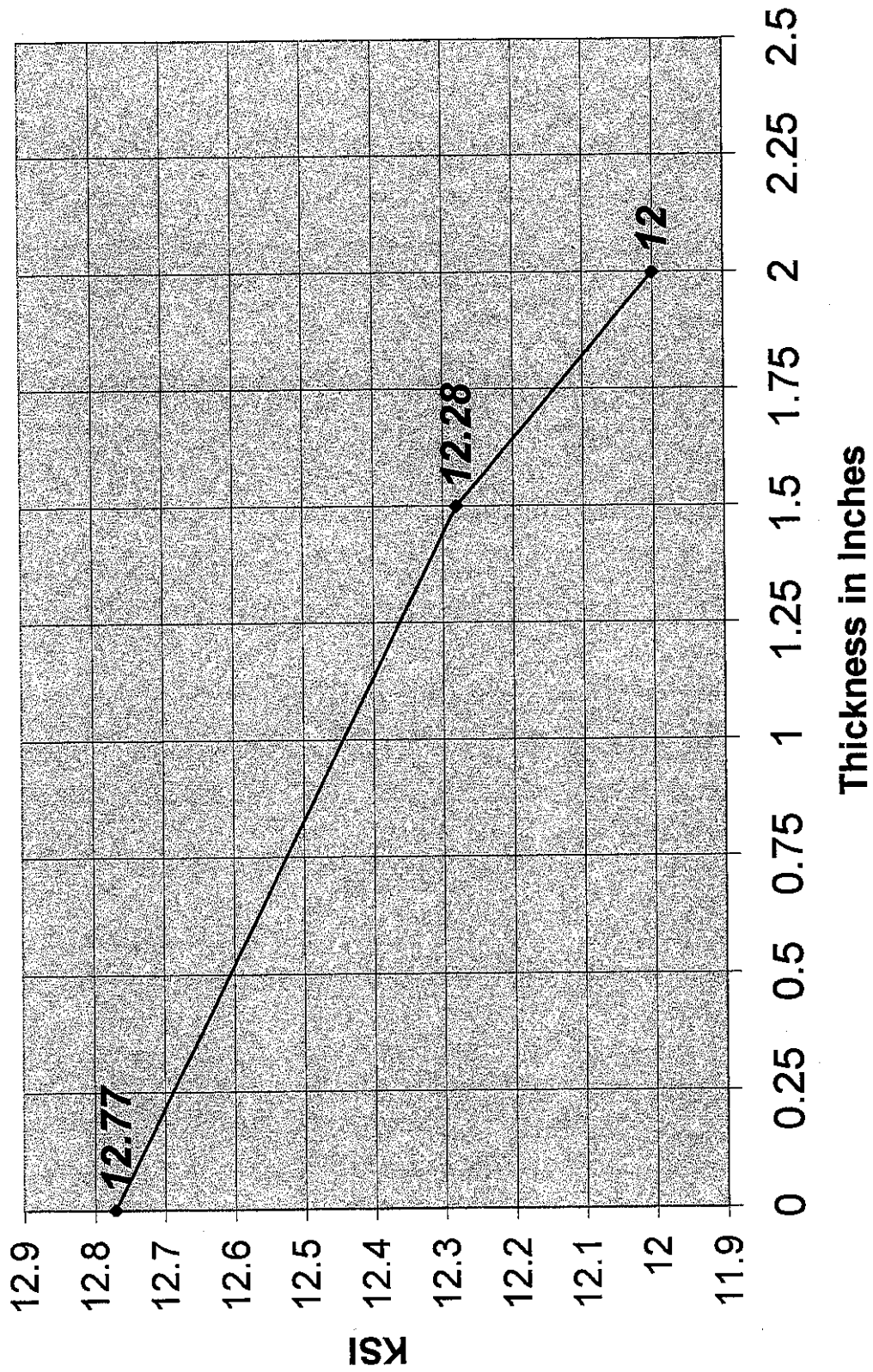
DATA NORMALIZED TO EMPTY TEST SPECIMEN FRAME

ORCON CORPORATION

3.75 Inch Thick Sprayed Panther Skin



Stress .VS. Thickness of Pantherskin



**FINITE ELEMENT STUDY OF AN AIRCRAFT
FUSELAGE WITH FOAM SUPPORT**

Submitted by

Professor. K.H. Wu

Dr. Tarek Lazghab

Florida International University

2002

TABLE OF CONTENTS

SECTION	PAGE
1 Executive Summary:	1
2 Introduction:	1
3 Description of the Model:	2
3.1 Components:.....	2
3.2 Material Properties:	3
3.3 Constraints & Element Types:	3
3.4 Boundary Conditions:	4
3.5 Results:	4
3.6 Fatigue Life:	5
4 Description of the Submodel:.....	6
4.1 Crack Length, Element types, Contours, etc:.....	7
4.2 J-Integral Calculations And Results:.....	7
4.3 Mode I Stress Intensity Factor (K_I):	8
4.4 Crack Growth:	8
5 Some Experimental Results:	10
5.1 FAA Fuselage Life Reduction.....	10
5.2 Deutsch Airbus Test.....	11
6 Conclusion:.....	11
7 Future Work:	12

LIST OF FIGURES

FIGURE	PAGE
Figure 1: Assembly drawing of the wing panel model without foam.....	16
Figure 2: Skeleton detail of the wing panel assembly.....	17
Figure 3: Outer Skin Assembly Detail of the Wing panel model	17
Figure 4: Stringer, Frame Tie Assembly Detail.	18
Figure 5: Foam layer applied to the inner side of the fuselage.	18
Figure 6: Foam Compressive Stress-Strain data	19
Figure 7: Foam Tensile Stress-Strain Data.	19
Figure 8: Boundary and loading conditions on the fuselage panel.	20
Figure 9: Percent reduction in hoop stress in noncracked fuselage vs. foam thickness....	20
Figure 10: Percent stress reduction in the noncracked fuselage vs. foam thickness.....	21
Figure 11: Percentage reduction in maximum radial deflection vs. foam thickness (noncracked fuselage).	21
Figure 12: Life increase in uncracked fuselage vs. foam layer thickness.	22
Figure 13: Mises stress distribution in Fuselage panel without foam (TOP).....	22
Figure 14: Mises Stress distribution in Fuselage Panel without foam (BOTTOM).....	23
Figure 15: Stress distribution in global fuselage model with a 2” thick foam layer.	23
Figure 16: Location of the Crack submodel in the global model of the fuselage section.	24
Figure 17: Global fuselage model with a crack in the skin (2” foam layer case).	24
Figure 18: Crack detail in the global Fuselage model.....	25
Figure 19: Collapsed Mesh of the Crack submodel	25
Figure 20: Deformed submodel with the driven DOF’s shown.	26

Figure 21: Crack submodel superimposed onto the crack in the global mode.	26
Figure 22: Stress distribution in the submodel (2" foam layer case).	27
Figure 23: Stress distribution at the crack tip (2" foam layer case).	27
Figure 24: J-integral path independence (Cracked fuselage).....	28
Figure 25: Percent reduction in J-integral vs. foam thickness (Cracked fuselage).	28
Figure 26: Percent reduction in K_I vs. foam thickness (Cracked Fuselage).....	29
Figure 27: Crack fatigue life increase vs. Foam thickness (Cracked fuselage).	29
Figure 28: Effect of additional foam layer on crack growth life (Experimental results compared vs. FEA).....	30

LIST OF TABLES

TABLE	PAGE
Table 1: Thickness of the components of the fuselage.	14
Table 2: Data collected at the most critical point of the fuselage skin.....	14
Table 3: Stress, values near rivets sites.	14
Table 4: Stability of J-integral value at different foam thicknesses.....	15
Table 5: Increase in fatigue life as a function of foam thickness noncracked fuselage.	15
Table 6: Increase in cycles to failure as function of foam thickness for the cracked fuselage.....	16

FAA Fuselage Panel Report

1 Executive Summary:

In the following report the effects of adding a foam layer of varying thickness was to skin of a fuselage section of an airplane were studied. The effects on fatigue life of the fuselage skin and crack growth rates were of special interest. A finite element model was built to estimate the effect of adding a foam layer on fatigue life and the stress and strain distributions in fuselage skin. The J-integral and the K_I stress intensity factor of a crack introduced in the fuselage skin were also calculated using a submodeling technique.

The foam layer thickness was varied from 0.5" to 4.0". It was found that fatigue life of the noncracked fuselage skin could be extended up to 48 times with a 4" thick foam layer. The stress intensity factor K_I was evaluated over the same range of foam layer thicknesses and corresponding crack growth rates were calculated from Paris law. It was determined that crack fatigue life could be reduced by a factor of 4.6 when a 4" thick foam layer is used.

Some experimentally obtained results compared against the numerical FEA results showed that the estimates from the model are twice as much as the experimental fatigue life data. This requires further studies to investigate the cause of the discrepancy.

2 Introduction:

Fatigue cracking is a major symptom of aging aircraft skin that could lead to widespread fatigue damage (WFD) in the fuselage structure of the aircraft. There are three major phases that lead to WFD, crack initiation, crack growth and crack

coalescence or crack link up which leads to fracture. The crack initiation mechanism involves high local stresses, fretting between mating surfaces and manufacturing defects during fuselage assembly.

Crack growth is affected by the loading configuration around the crack represented qualitatively by the stress intensity factor, the number of elapsed cycles, the amplitude of the loading at each cycle, the frequency of the cycles and the material properties.

Several strategies can be used to extend the fatigue life of a structure. This can be done by reducing operating loads, reinforcing the structure to reduce stresses, introducing residual stress that stunt crack growth, special material treatment, etc.

In the current report, it is proposed to use foam as a reinforcing material to mitigate the stress distribution on the fuselage skin and help extend the useful life of the aircraft. The foam is applied to the inner side of the skin to several foam thickness levels and the resulting effects on the structure are evaluated numerically using a finite element approach. In addition, a study of the effects of the foam on stress concentration characteristics around a crack in the fuselage skin is conducted.

3 Description of the Model:

3.1 Components:

The original finite element model was received from the FAA in the form of a ANSYS input file. This file was reverse engineered and rebuilt into ABAQUS format. The model represents a fuselage panel cutout from a commercial airliner. Figures 1 thru 4 illustrate the components of the fuselage panel and the assembly detail. The components of the fuselage panel (Stringers, frames, fillers, skins, ties, etc...) are held together by

rivets (not shown). In the original model the rivets are represented by short beam elements in the current model the rivets were replaced by a tied contact that acts as a strong adhesive between components. All the components are made from aluminum. The ties, stringers and frame all provide reinforcement and a load transfer path to the fuselage skin.

In the current study the foam is added to the inner side of the fuselage section as shown in Figure 5. Different foam thicknesses will be modeled in order to evaluate their effect on the stress distribution in the skin of the fuselage section.

3.2 Material Properties:

The materials used in the fuselage assembly are aluminum and foam. The aluminum is assumed to be operating within its elastic limit with the following elastic material properties.

Aluminum: $E_A=10. \text{ Msi}$ $\nu_A=0.33$

Foam: $E_F=3000. \text{ psi}$ $\nu_F=0.3$

The plastic stress-strain response of the foam (tension and compression) is given in Figure 6 & Figure 7.

3.3 Constraints & Element Types:

The aluminum components of the fuselage are modeled using 4 node reduced integration linear shell elements (S4R). The rivets are not represented in the FEA model. Instead the assembly between components is insured by implementing constraints between degrees of freedom of the contact regions of the components forcing the displacements to be equal and thus simulating the assembly constraint.

The foam is represented using continuum 8-node reduced integration solid elements where the displacements are constrained to those of the skin of the fuselage at the contact interface between the foam and the skin. The foam was modeled at several thicknesses (1.5", 2.0", 2.5", 3.0", 3.25", 3.5" and 4.0"). The model has 14385 elements and 56228 nodes.

3.4 Boundary Conditions:

The loading and boundary conditions on the fuselage section are shown in Figure 8. A line load is applied to *Edge3* to account for the stresses generated by cabin pressure during flight. Not shown in the figure is a distributed pressure load on the inner surface of the foam due to cabin pressure also. The cabin pressure load is stepped from 0 to 7. *psi*. The line load magnitude is a function of the cabin pressure and is given by

$$F = \frac{1}{2} P.R^2\phi \quad (1)$$

Where R is the radius of at the skin of the fuselage panel, P is the cabin pressure and ϕ is the angle subtended by the fuselage section around the Z axis in radians as shown in Figure 8. The geometry of the fuselage section and the loading conditions yield the following values for the parameters from Eq. (1):

$$R= 74.018 \text{ in}; \phi=37.164 \text{ deg} = 0.649 \text{ radians}; P=7.0 \text{ psi} \ \& \ F= 12436 \text{ lbf.}$$

3.5 Results:

The fuselage structure was modeled using several foam thicknesses given in Table 2. To illustrate the effect of applying foam to the fuselage skin, the stress-strain data was collected from the point of maximum stress in the aluminum skin for different

foam thicknesses (data collected is Hoop strain, hoop stress and radial displacement). The data collected is plotted vs. foam thickness. Graphically it can be seen in Figure 9 through Figure 11 that additional foam thickness helps reduce the stress and strain levels and the maximum displacements in the radial direction by up to 25% at 4" foam thickness level. This will have direct impact on extending the fatigue life of the fuselage. Table 2 presents the data obtained. In Figure 13 and Figure 14 a typical stress distribution in the Fuselage panel section without foam is shown. It can be seen that the skin has the highest stress level in the structure indicating that is more vulnerable to fatigue than other components. Figure 15 shows the stress distribution in the fuselage skin with 2" layer applied it can be seen that the stress levels were reduced significantly in the skin. Moreover, the stress gradients are more benign indicating a more uniform stress distribution that is less conducive to stress concentrations and therefore crack initiation.

The stress and strain levels were also sampled at the site of the riveted straps where the stresses are expected to be high due to the presence of rivets (modeled as tie constraints in the model). It was found that stress and the strain were reduced by 24% when a 4" thick foam layer is applied. Table 3 presents the stress strain data obtained for the most critical point of the fuselage skin near the rivets.

3.6 Fatigue Life:

The fatigue life for the fuselage skin is given by the Coffin-Manson equation:

$$\frac{\Delta \epsilon}{2} = \frac{\sigma_f}{E} (2N_f)^b + \epsilon_f' (2N_f)^c \quad (2)$$

Where

$\Delta\varepsilon$: Strain range.

$\left(\frac{\sigma_f'}{E}\right) = .008632$: On reversal intercept of elastic strain vs. life line.

$\varepsilon_f' = 0.18$: One reversal intercept of plastic strain vs. life line.

$b = -.071$: Slope of elastic strain amplitude vs. fatigue life.

$c = -.645$: Slope of plastic strain amplitude vs. fatigue life.

N_f : Cycles until failure.

The numerical values for the constants are obtained for aluminum, which is the material of the fuselage skin.

Fatigue life for the uncracked fuselage was evaluated at the location of maximum stress and strain. The fatigue life extension results are given in Table 5. The effect of the foam layer thickness on fatigue life at the critical point is depicted in Figure 12.

4 Description of the Submodel:

In order to estimate the effect of the foam layer thickness on fatigue life of the fuselage section a 4.5" crack is introduced in the global mesh of the fuselage section. The region neighboring the crack is further analyzed using a submodel. Figure 16 shows the location of the submodel with respect to the global model of the fuselage section.

First the crack is introduced in the global model at the desired location by modifying the mesh of the global model. The stress distribution of the cracked global model is then obtained as shown in Figure 17 and Figure 18 for the case of a 2" foam layer.

In a second step the global model is superimposed onto the location of the existing crack in the global model and displacements are interpolated from the aluminum skin and

the foam in the vicinity of the crack. These displacements are in turn used in the submodel to calculate the J-integral at the stress intensity factors tip.

4.1 Crack Length, Element types, Contours, etc:

The mesh for the crack submodel is shown in Figure 19, it is made up of the quadratic 20-node continuum elements with biased mid-nodes of the elements at the crack tip. The nodes at the crack front are tied and constrained to move together. The combination of biased mid-nodes and tied nodes at the crack tip produce a strain field singularity proportional to $\frac{1}{\sqrt{r}}$ where r is the distance from the crack tip. The mesh is parameterized and allows for a variable number of integration contours around the crack tips. In this case, 10 contours around each crack tip are used for the calculation of the J-integral. The boundary conditions are interpolated from the boundary nodes of the submodel mesh. These nodes are called the driven nodes. In this case the driven nodes are located on the perimeter of the aluminum skin in the through the thickness direction as shown in Figure 20. A pressure load of 7 *psi* is still applied to the section of the foam in the submodel. Nodes at the Aluminum/Foam interface are shared by adjacent elements from both materials. Figure 22 through Figure 23 illustrate a typical stress distribution in the submodel and at the crack tip.

4.2 J-Integral Calculations And Results:

The J-integral was calculated along 10 contours at the crack tip. This is standard practice in FEA to ensure that the value of the J-integral is path independent. Table 4 presents numerical values of the J-integral value along different contours and for several foam thicknesses. The values of J-integral were at most within 6% of each other for

different contour paths. The virtually constant value of the J-integral in Figure 24 illustrates its independence from the path of integration.

The percent reduction in the value of the J-integral as a function of the foam layer thickness is shown in

Figure 25. Applying foam of thickness up to 4" can reduce the J-integral value down to 60% of its value when no foam is applied. The trend obtained is fit to a 4th order polynomial.

4.3 Mode I Stress Intensity Factor (K_I):

The stress intensity factors were also evaluated from the model at the crack tips for several foam layers. The percentage reduction of K_I vs. foam thickness is shown in Figure 26, reduction of up to 35% in K_I can be achieved. The data trend obtained is fit to a 4th order polynomial equation and is also shown in Figure 26.

4.4 Crack Growth:

Paris law gives the crack growth rate as follows:

$$\frac{da}{dN} = A(\Delta K)^m \quad (3)$$

Where a is the current crack length, N is the number of cycles, ΔK is the stress intensity factor range and A and n are material constants. For the current study the values of these constants are $A = 2.5E-12$ and $m = 3.5$. To evaluate the impact of the foam on the crack growth rate consider the following expressions

$$\left(\frac{da}{dN}\right)_A = C(\Delta K_A)^m \quad (a)$$

$$\left(\frac{da}{dN}\right)_F = C(\Delta K_F)^m \quad (b) \quad (4)$$

$$\frac{\Delta K_A - \Delta K_F}{\Delta K_A} = p \quad (c)$$

Where

ΔK_A : stress intensity factor range for the aluminum skin without foam.

ΔK_F : stress intensity factor range for the aluminum skin with a foam layer.

$\left(\frac{da}{dN}\right)_A$: Crack growth rate for aluminum skin only.

$\left(\frac{da}{dN}\right)_F$: Crack growth rate for aluminum skin with foam.

The cycle to failure for the aluminum skin with foam are given by:

$$(N_f)_F = \int_0^{N_f} dN = \int_{a_0}^{a_c} \frac{da}{C(\Delta K_F)^m} \quad (5)$$

Solving for ΔK_F in Eq. (4)-a and substituting into Eq. (5) yields:

$$\begin{aligned} (N_f)_F &= \int_{a_0}^{a_c} \frac{da}{C(\Delta K_F)^m} = \int_{a_0}^{a_c} \frac{da}{C(\Delta K_A(1-p))^m} = \frac{1}{(1-p)^m} \int_{a_0}^{a_c} \frac{da}{C(\Delta K_A)^m} \\ &= \frac{1}{(1-p)^m} (N_f)_A \end{aligned}$$

Therefore:

$$(N_f)_F = \frac{1}{(1-p)^m} (N_f)_A \quad (6)$$

The addition of the foam has increased the number of cycles to failure by a factor of

$$\frac{1}{(1-p)^m}; (0 < p < 1.0)$$

The effect of foam thickness on crack fatigue life is shown in Figure 27. Table 6 presents the numerical results of the increase in crack fatigue life as a function of foam thickness. At 4" foam thickness life can be extended as much as 4.78 times.

Using a similar argument as above it can be shown that for given number of cycles N and an initial crack length a_0 the following relation holds:

$$(a_c^F - a_0) = (1-p)^m (a_c^A - a_0) \quad (7)$$

Where a_c^F is the final crack length in the foam/aluminum assembly and a_c^A is the final crack length in the aluminum fuselage alone. The crack growth for a given number of cycles N is $(1-p)^m$ times smaller in the foam/aluminum assembly than in the aluminum assembly alone.

5 Some Experimental Results:

5.1 FAA Fuselage Life Reduction

The FAA has conducted Crack growth tests in 1999 on a fuselage section 0.05" thick with a 2.75" long crack under a 5 psi cyclic load. The crack was allowed to grow up to 3.5" in length. The number of cycles needed to reach the final crack length was 4000 cycles. The same test was repeated with an added 3.5" thick foam layer added to the skin. The number of cycles needed to reach a 3.5" crack length jumped to 12000 cycles. A 2-fold increase in crack growth life was achieved. The experimental test conditions were

replicated in the FEA model to estimate the crack growth life fold increase. The estimate from the FEA model yields a 5-fold increase in the fatigue as shown in Figure 28. It is important to mention that these results are strongly dependent on the exponent n in Paris law as indicated in Eqs. (3) and (6).

5.2 Deutsch Airbus Test

Deutsch Airbus has conducted experimental tests on 10 cm crack with 2.5" thick foam layer it yielded a reduction in crack growth rate $\left(\frac{da}{dN}\right)$ of 50%. Under Similar loading conditions the FEA model has yielded a reduction in crack growth rate of 24.5%.

6 Conclusion:

A study on the effect of bonding a foam layer to the fuselage skin of an airplane was considered. The stress distribution, fatigue life, and crack growth rates of the fuselage skin were evaluated using the finite element method. It is found that applying a foam layer to the inner surface of the fuselage skin helps reduce the stress levels by up to 25% in areas of maximum stress and near the riveted lap joints. The maximum, stress, strain and deflection values were reduced by an average 26% of their base values when no foam is used.

The effect of the additional foam layer on fatigue life as calculated according to Coffin-Manson law indicated that an 48-fold increase could be achieved with a 4" thick foam layer.

A submodel was built to analyze the effects of the foam on fatigue life of the aluminum fuselage when a crack is present in it. It was determined that the stress

intensity factor (Mode I) can be reduced by 36% for a 4" thick foam layer which translates into an increase in fatigue life by up to 4.78 folds.

Experimentally obtained fatigue life data were compared to results obtained from the finite element model. The outcome showed that the model is within 50% of the experimental results this discrepancy is attributed to the strong dependence of the theoretical result on the exponent n in Paris' equation. Since the value of this parameter is not available from the experimental data only an estimated value is used.

7 Future Work:

In this study the effect of adding foam were studied using a finite element approach. The stress intensity factors were evaluated directly. During the calculation of the J-integral and the stress intensity factors at the crack tips several numerical issues were encountered namely, unstable and path dependent J-integral values at the Aluminum/Foam interface. The approach used to model the interface between the two materials can affect the J-integral and the K_I stress intensity factor significantly. The approaches used were (1) Tie constraints between the aluminum and the foam faces; (2) contact formulation and using (3) shared nodes between the foam and the aluminum faces. Even though the shared nodes approach proved to be the most effective it is still necessary to ensure that which of these approaches simulates the fuselage and loading conditions most accurately.

In the current study contour integration was used in the evaluation of the J-integral and the K_I stress intensity factor. The results obtained must be reproduced using alternate methods such as Virtual Crack Extension, Strain Energy Release Rate, etc.

The current finite element package used ABAQUS does not account for pressure loads in the calculation of the J-integral and K_I . Furthermore, curvature of the shell elements contributes in the degradation in the accuracy of the values for J-integral and K_I . To avoid this pitfall the submodel was built entirely of continuum quadratic elements. However, in order to obtain more accurate results special purpose software such as FASTRAN, FRANC3D, etc might be necessary.

Ultimately experimental validation of the finite element model to characterize the trends established by the FEA model needs to be conducted in order to assert the effects of various foam thicknesses on the fatigue life of the fuselage skin. In addition, a study to determine the optimal foam thickness that provides maximum life extension and minimal cost and weight increase is a necessary step before implementation.

Table 1: Thickness of the components of the fuselage.

Component	Thickness (in)
Bottom Skin	0.036
Straps	0.04
Top Skin	0.036
Fillers	0.04
Stringers	0.05
Ties	0.05
Frame	0.05
Gussets	0.04

Table 2: Data collected at the most critical point of the fuselage skin.

Foam Thickness (in)	Stress	Strain	Displacement	Pct Stress Reduction	Pct Strain Reduction	Pct Disp. Reduction
	(ksi)	(%)	(in)			
0	12.373	1.1581	0.0857	0.0%	0.0%	0.0%
0.25	12.233	1.1481	0.085	1.1%	0.9%	0.9%
0.5	11.887	1.124	0.0832	3.9%	2.9%	2.9%
1	10.876	1.0524	0.0779	12.1%	9.1%	9.1%
1.5	10.623	1.0069	0.0745	14.1%	13.1%	13.1%
2	9.875	0.9721	0.072	20.2%	16.1%	16.1%
2.5	9.814	0.948	0.0702	20.7%	18.1%	18.1%
3	9.449	0.9289	0.0688	23.6%	19.8%	19.8%
3.5	9.704	0.9147	0.0677	21.6%	21.0%	21.0%
4	9.16	0.9016	0.0667	26.0%	22.1%	22.1%

Table 3: Stress, values near rivets sites.

Foam Thickness (in)	Stress (ksi)	Strain (*1E-6)
0.00	12.164	1384.4
4.00	9.1601	1050.31
Pct Reduction	24.70%	24.13%

Table 6: Increase in cycles to failure as function of foam thickness for the cracked fuselage.

Foam Thickness (in)	Percent reduction in ΔK_I	Life increase fold
0.00	0.0%	1.00
0.50	11.2%	1.52
1.50	29.1%	3.32
2.00	28.6%	3.24
2.50	33.1%	4.09
3.00	34.3%	4.35
3.50	35.1%	4.53
4.00	36.0%	4.78

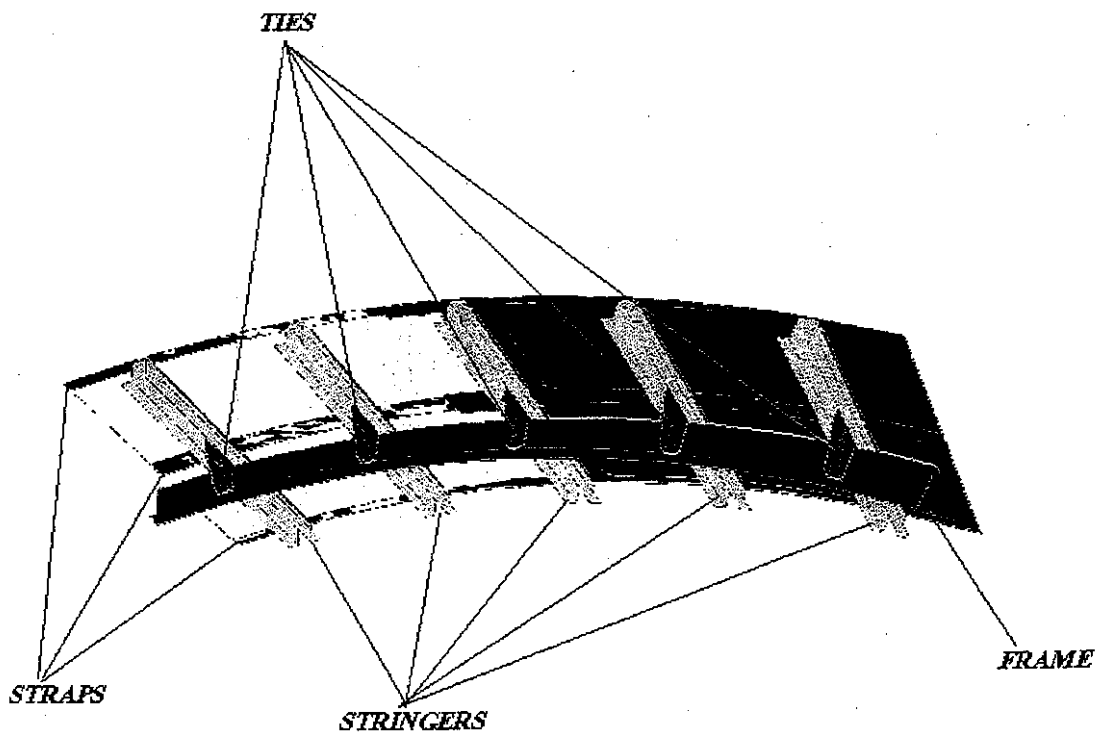


Figure 1: Assembly drawing of the wing panel model without foam.

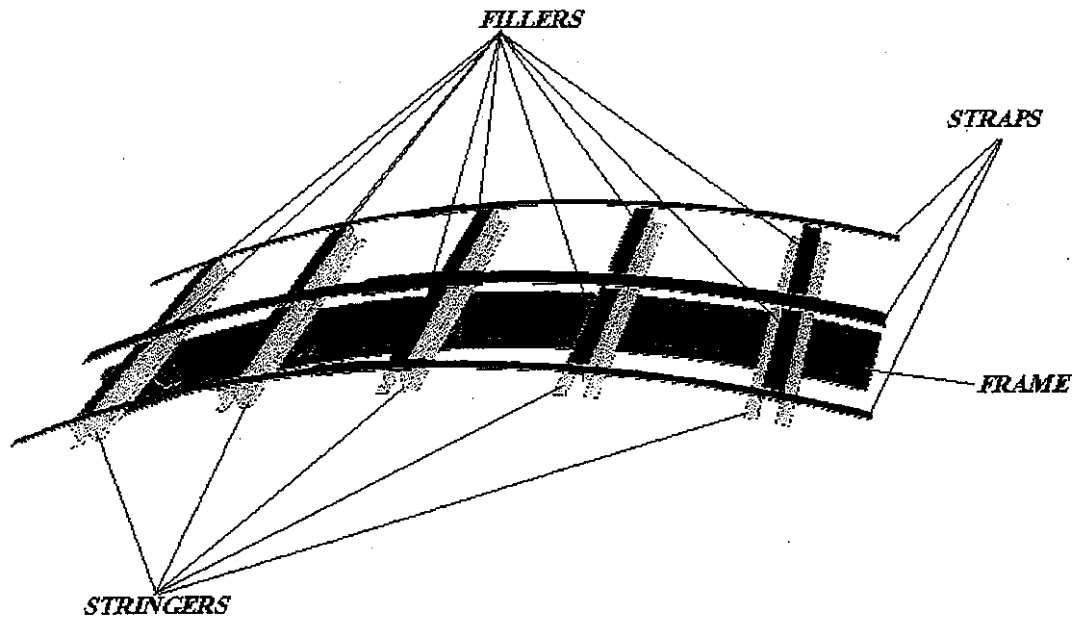


Figure 2: Skeleton detail of the wing panel assembly

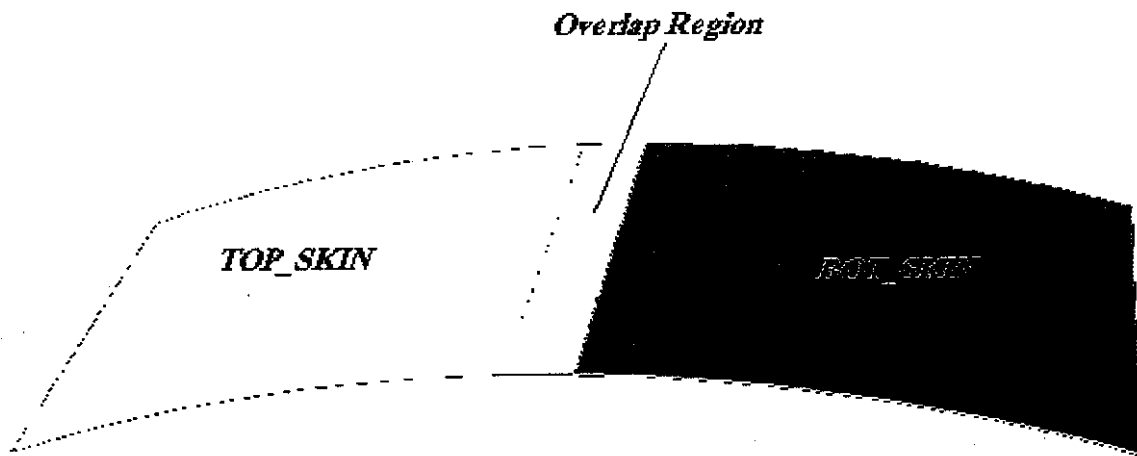


Figure 3: Outer Skin Assembly Detail of the Wing panel model

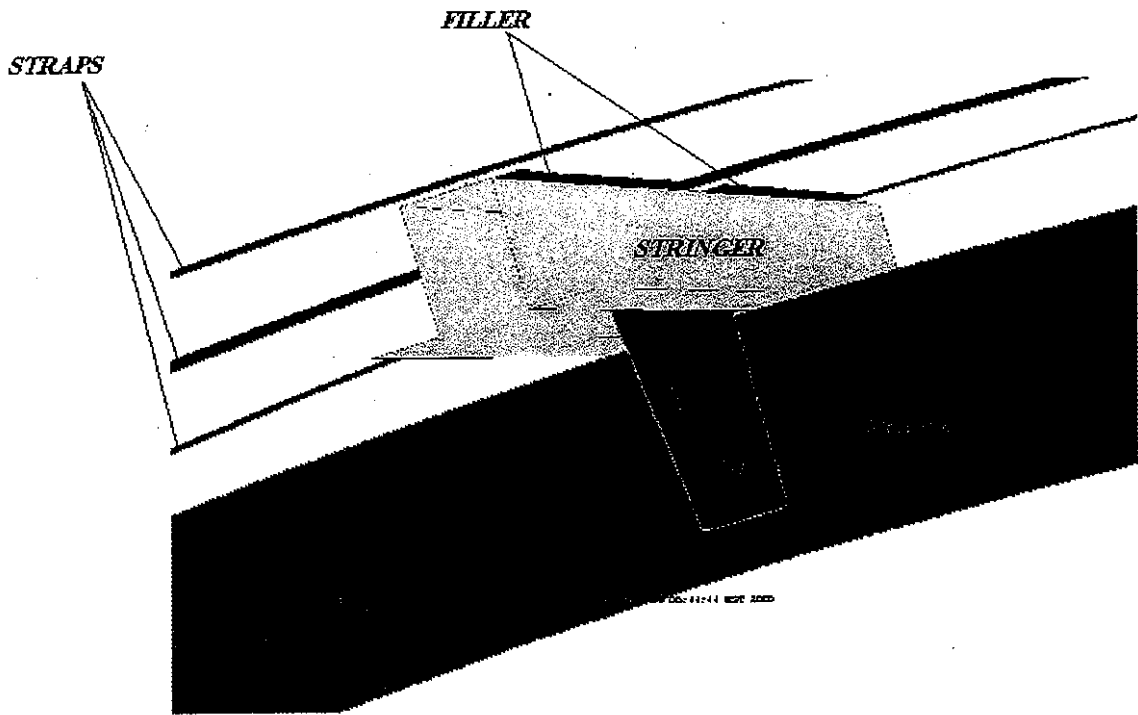


Figure 4: Stringer, Frame Tie Assembly Detail.

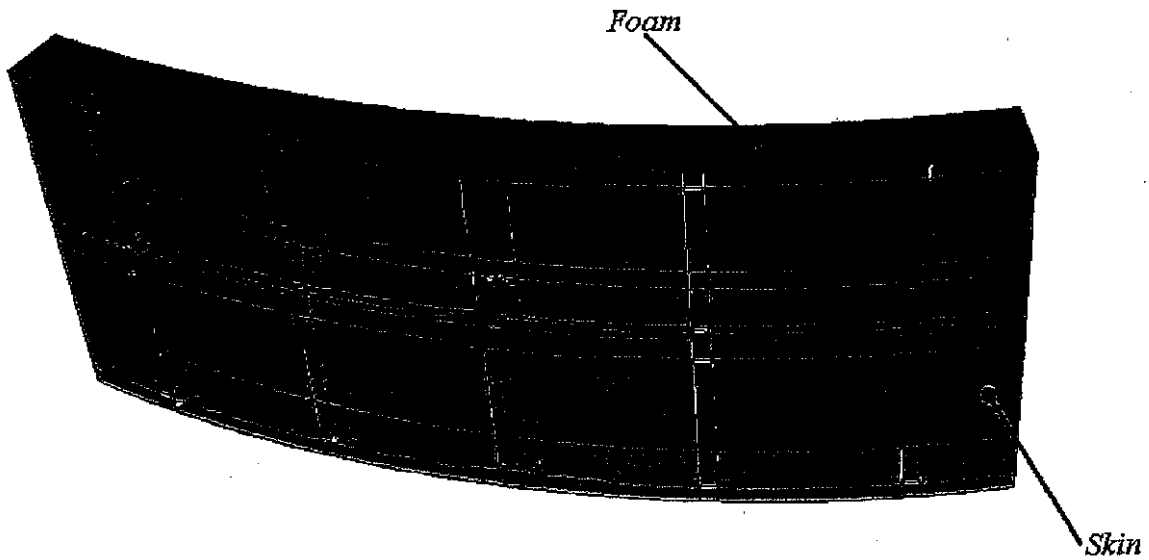


Figure 5: Foam layer applied to the inner side of the fuselage.

STRESS vs. STRAIN for COMPRESSIVE TEST

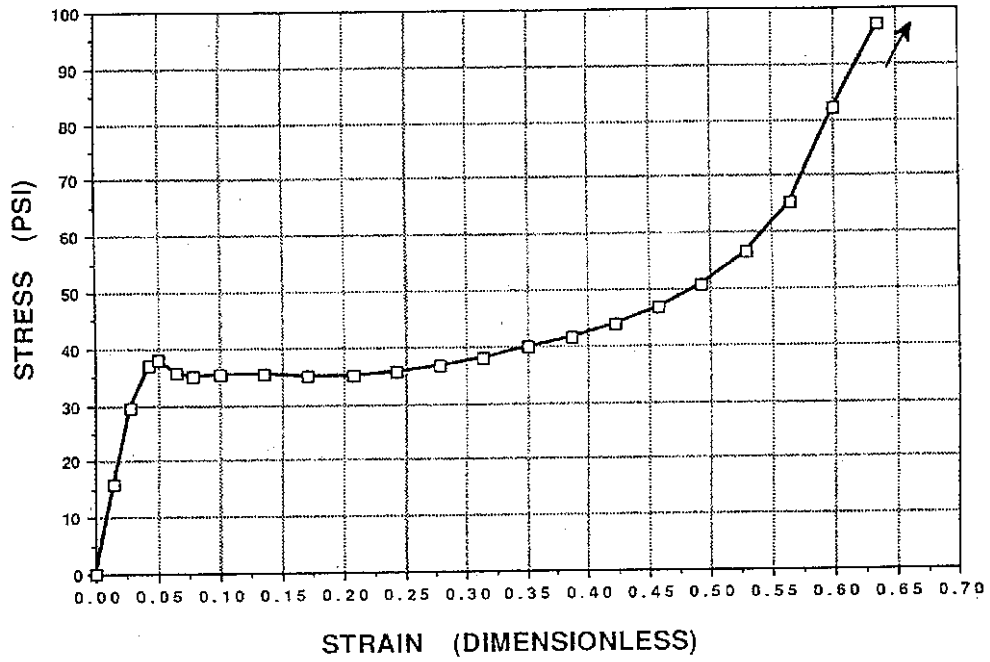


Figure 6: Foam Compressive Stress-Strain data

STRESS vs. STRAIN for TENSILE TEST

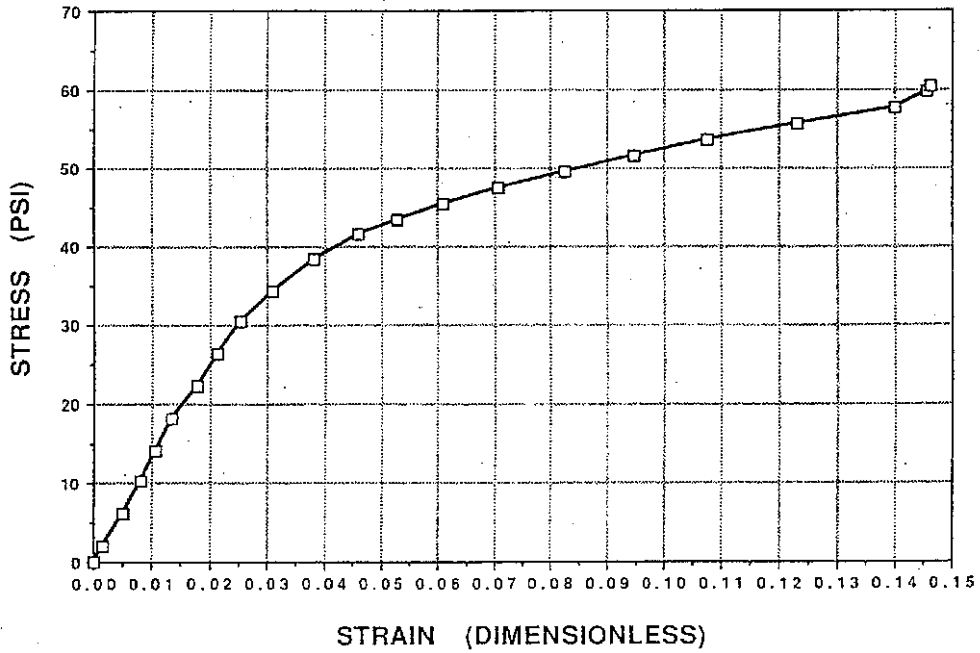


Figure 7: Foam Tensile Stress-Strain Data.

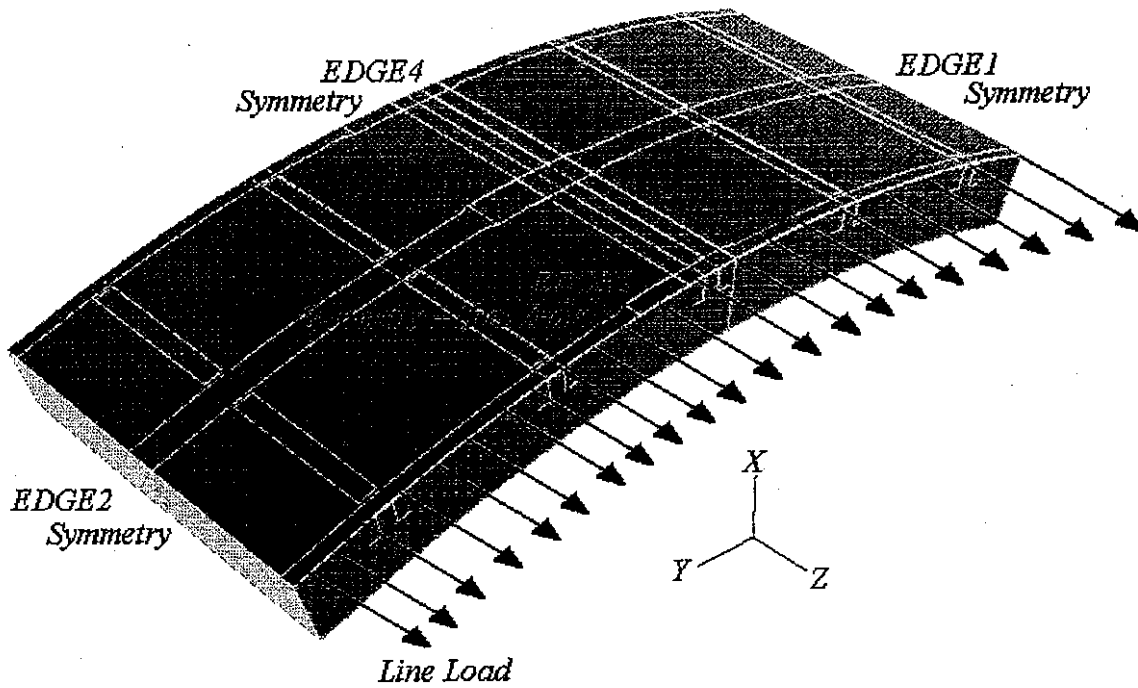


Figure 8: Boundary and loading conditions on the fuselage panel.

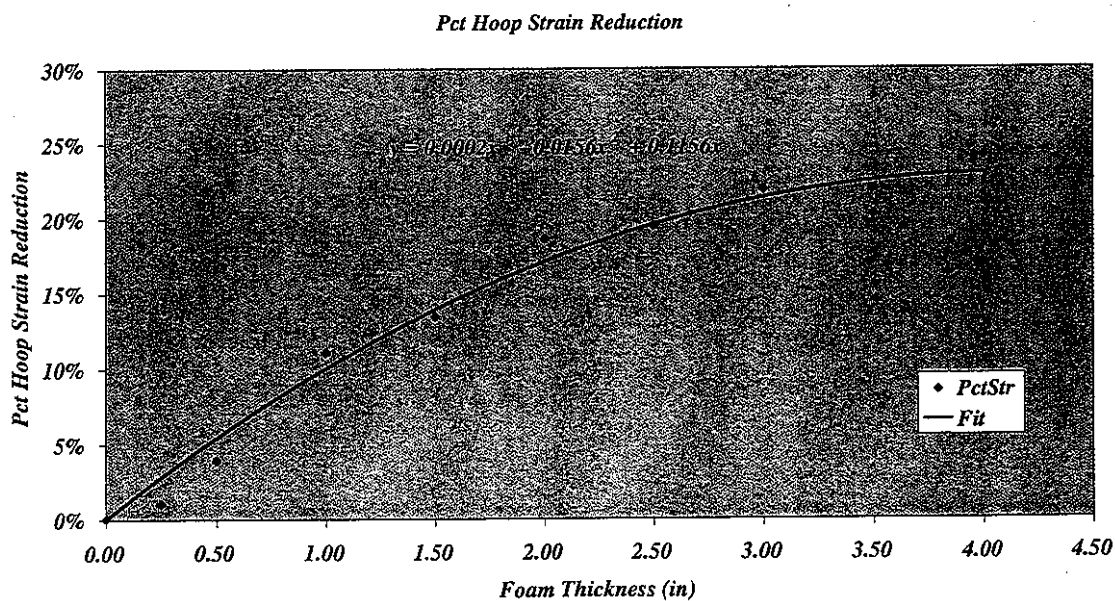


Figure 9: Percent reduction in hoop stress in noncracked fuselage vs. foam thickness.

Percent Stress reduction vs. Foam Thickness

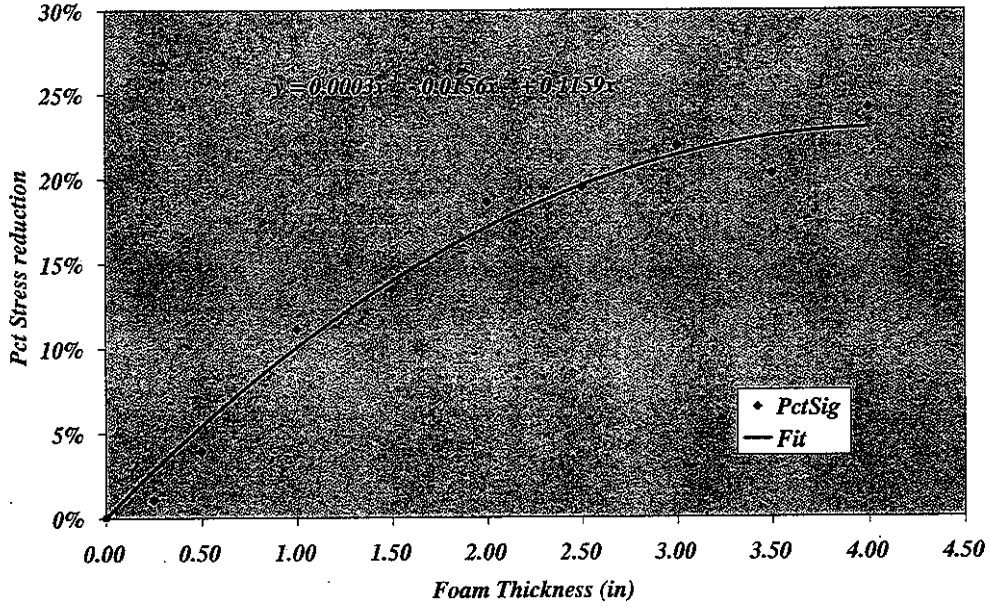


Figure 10: Percent stress reduction in the noncracked fuselage vs. foam thickness.

Percent Radial Displacement Reduction

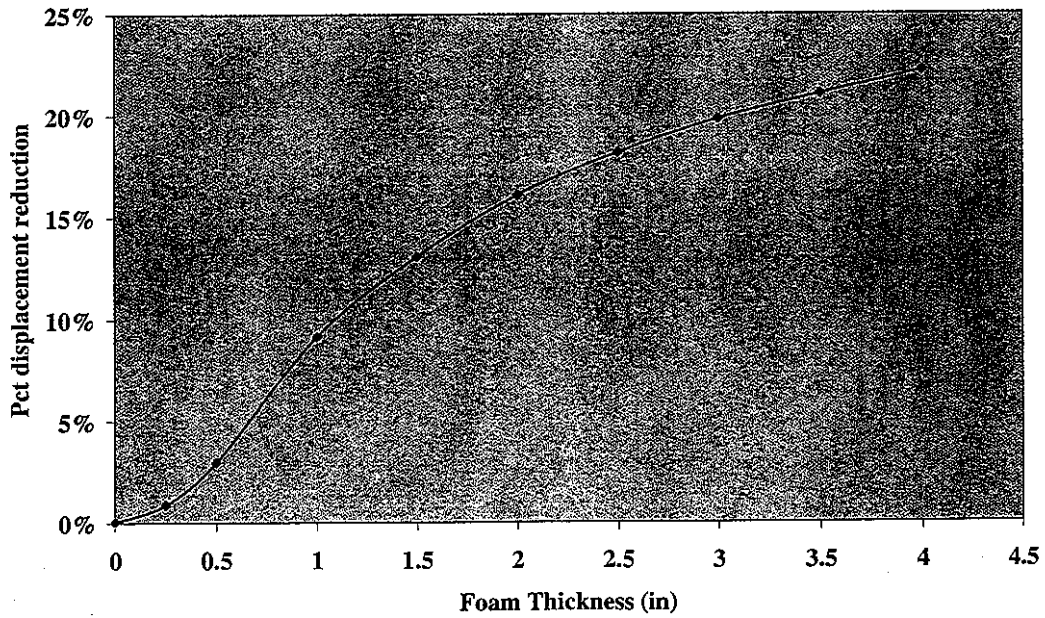
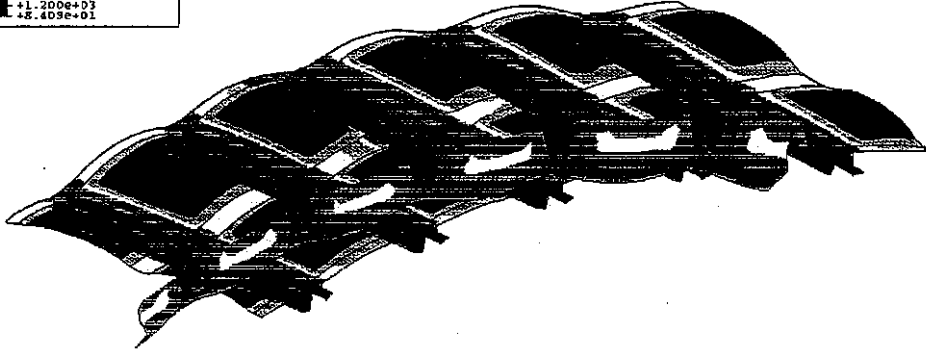


Figure 11: Percentage reduction in maximum radial deflection vs. foam thickness (noncracked fuselage).

S, Mises
 SPOS, (fraction = 1.0)
 (Ave. Crit.: 75%)

█	+1.348e+04
█	+1.238e+04
█	+1.128e+04
█	+1.018e+04
█	+9.018e+03
█	+7.918e+03
█	+6.782e+03
█	+5.658e+03
█	+4.548e+03
█	+3.438e+03
█	+2.317e+03
█	+1.200e+03
█	+5.409e+01



ODB: jFuselage_NF_NC.odb ABAQUS/Standard 5.2-1 Tue Oct 23 10:03:04 EDT 2001

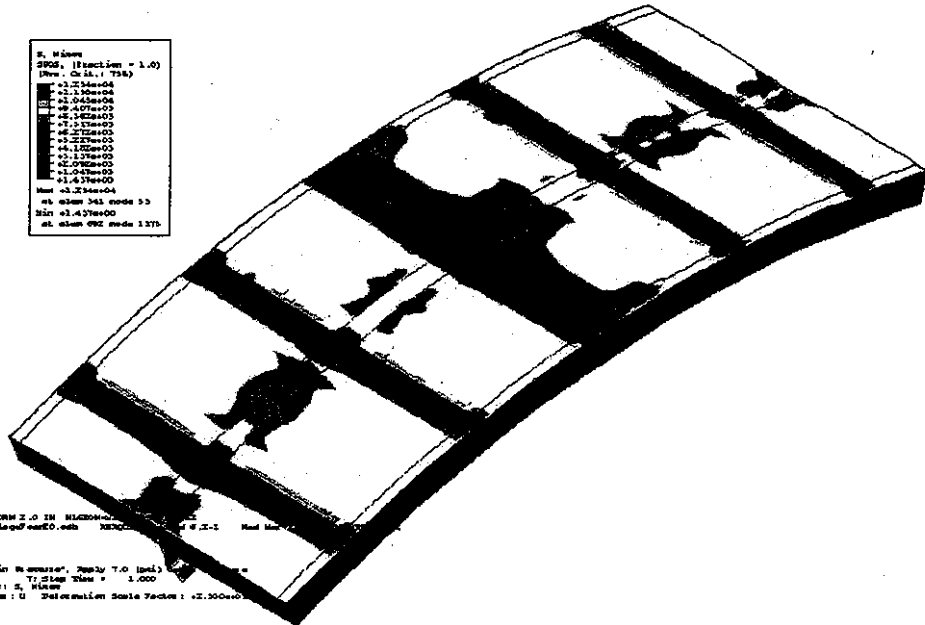
Step: Step-3, PressurizeCabinet: Pressurize Cabinet to 8.5 Psi
 Increment 1; Step Time = 1.000
 Primary Var: S, Mises
 Deformed Var: U Deformation Scale Factor: +5.000e+01

Figure 14: Mises Stress distribution in Fuselage Panel without foam (BOTTOM).

S, Mises
 SPOS, (fraction = 1.0)
 (Ave. Crit.: 75%)

█	+2.234e+04
█	+2.124e+04
█	+2.014e+04
█	+1.904e+04
█	+1.794e+04
█	+1.684e+04
█	+1.574e+04
█	+1.464e+04
█	+1.354e+04
█	+1.244e+04
█	+1.134e+04
█	+1.024e+04
█	+9.14e+03
█	+8.04e+03
█	+6.94e+03
█	+5.84e+03
█	+4.74e+03
█	+3.64e+03
█	+2.54e+03
█	+1.437e+00

Max at 234e04
 at elem 341 node 33
 Min at 1.437e00
 at elem 992 node 1378



PATRAN FORM 2.0 IN MICRO...
 ODB: jFuselage_Foam20.odb
 Step: "Cabin Pressure", Step 7.0 (end)
 Increment 7; Step Time = 1.000
 Primary Var: S, Mises
 Deformed Var: U Deformation Scale Factor: +2.500e+01

Figure 15: Stress distribution in global fuselage model with a 2" thick foam layer.

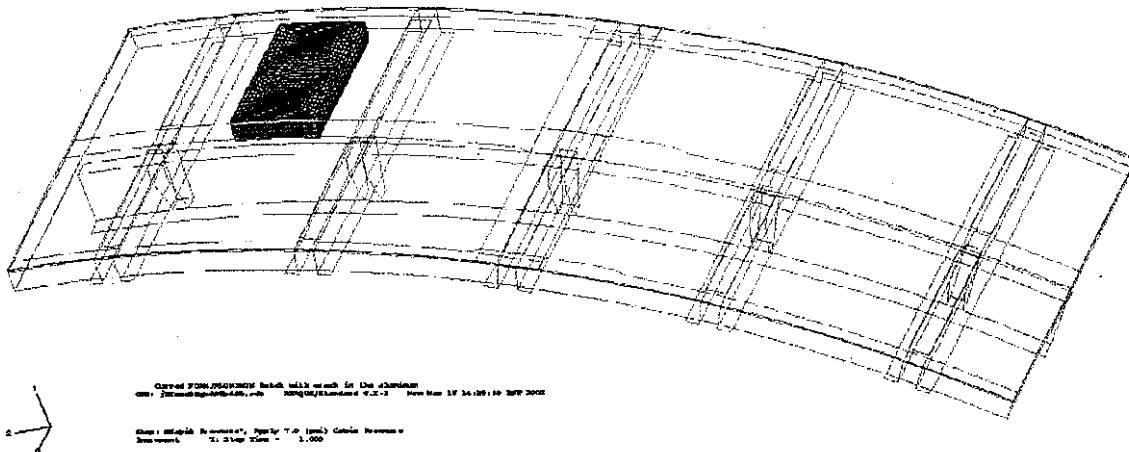


Figure 16: Location of the Crack submodel in the global model of the fuselage section.

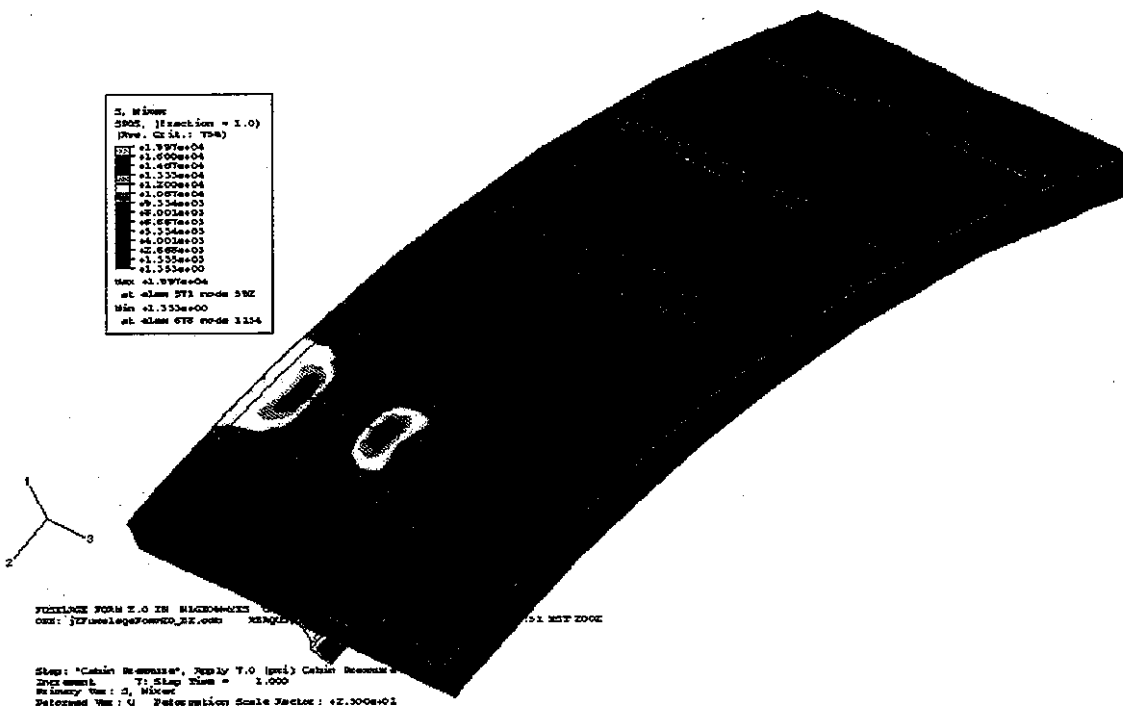


Figure 17: Global fuselage model with a crack in the skin (2" foam layer case).

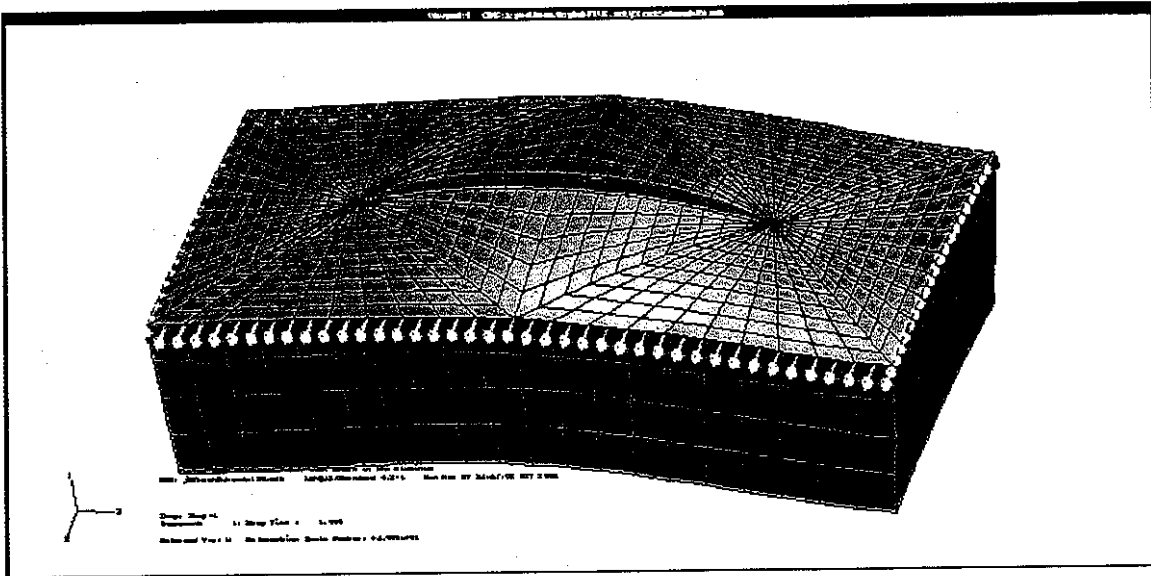


Figure 20: Deformed submodel with the driven DOF's shown.

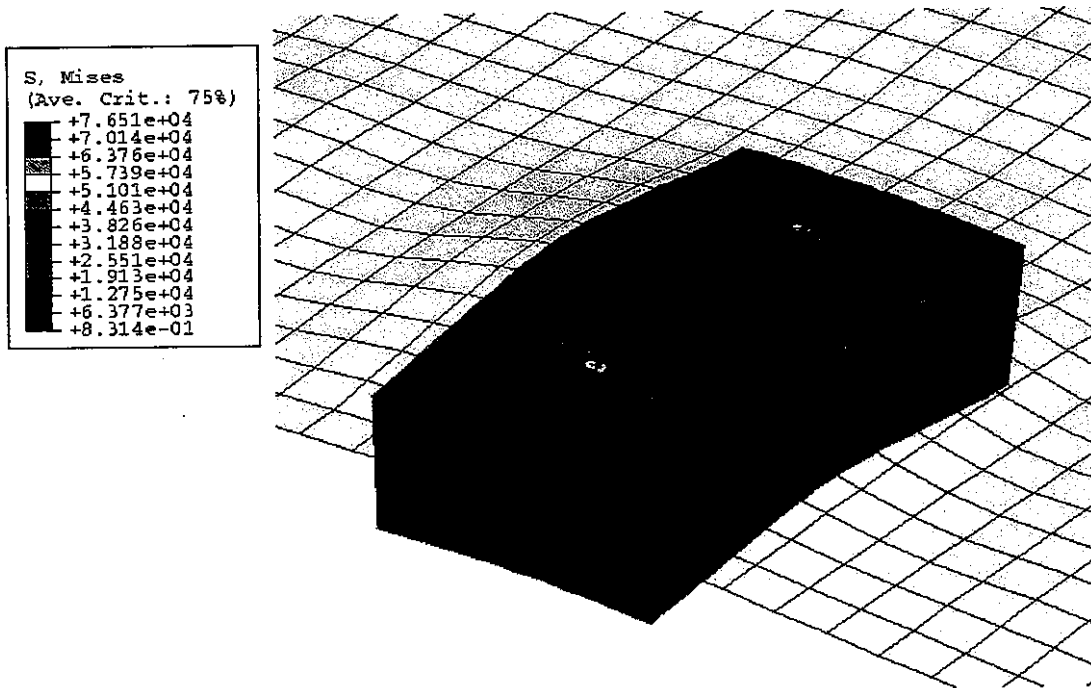


Figure 21: Crack submodel superimposed onto the crack in the global mode.

J-Integral Path independence

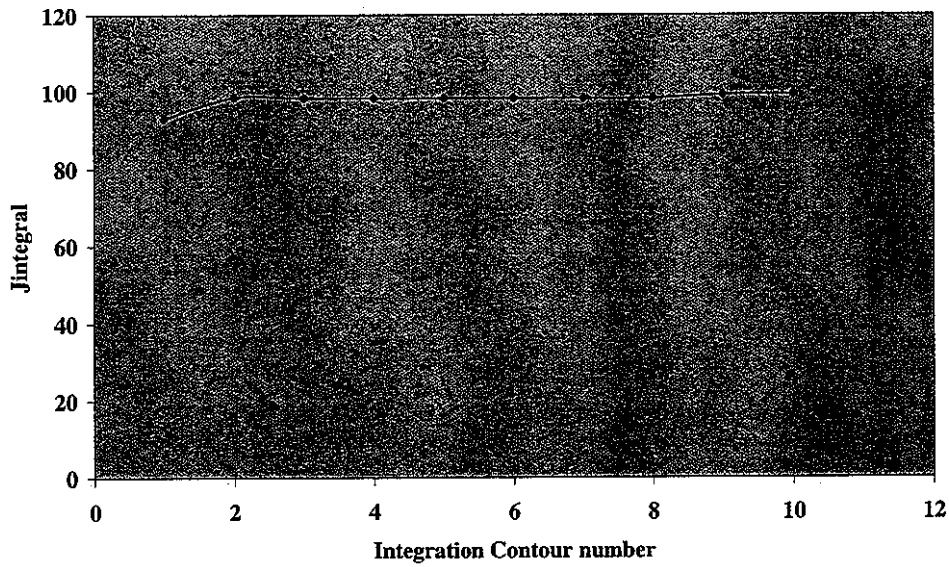


Figure 24: J-integral path independence (Cracked fuselage)

J-integral Percent Reduction vs. foam thickness

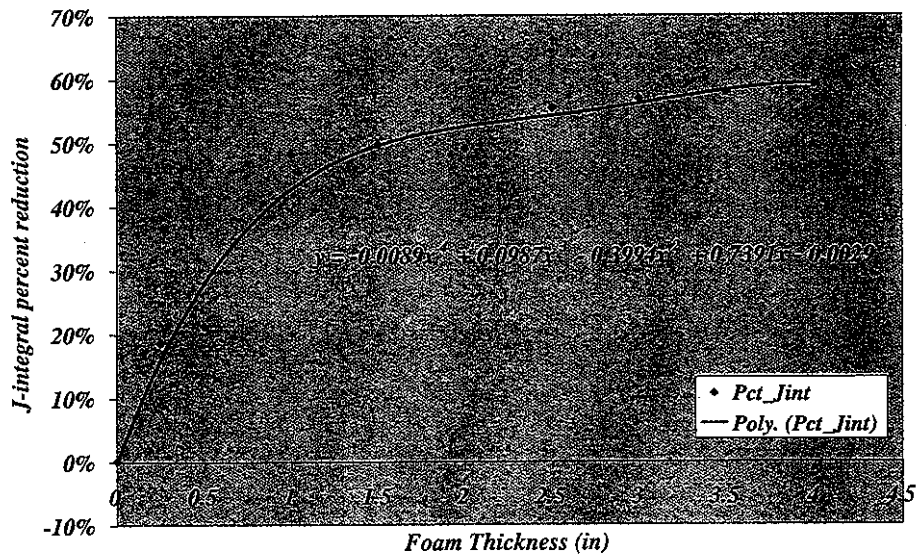


Figure 25: Percent reduction in J-integral vs. foam thickness (Cracked fuselage).

Percent K1 reduction vs. foam thickness

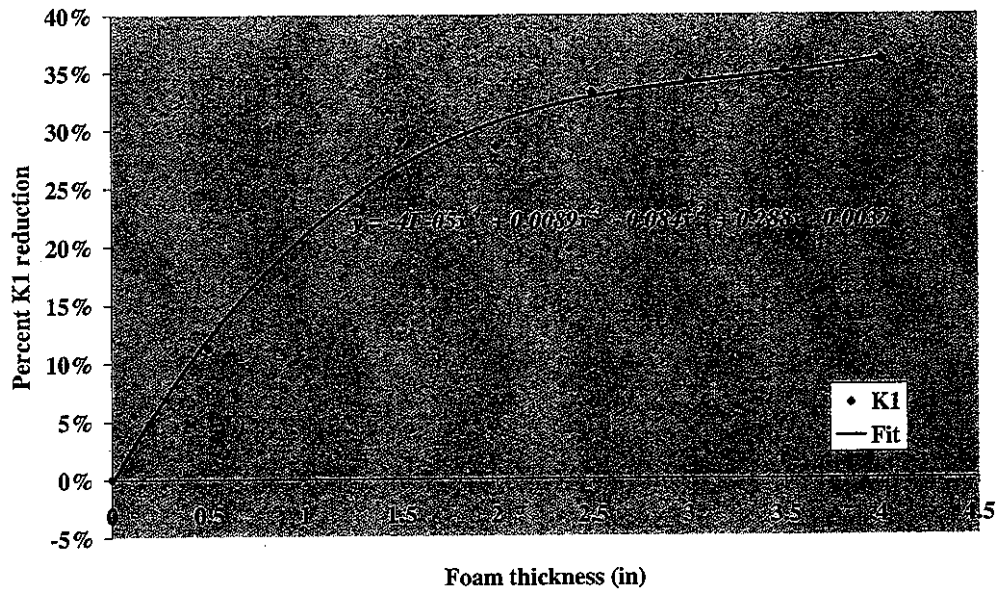


Figure 26: Percent reduction in K_I vs. foam thickness (Cracked Fuselage)

Crack Fatigue Life Fold increase

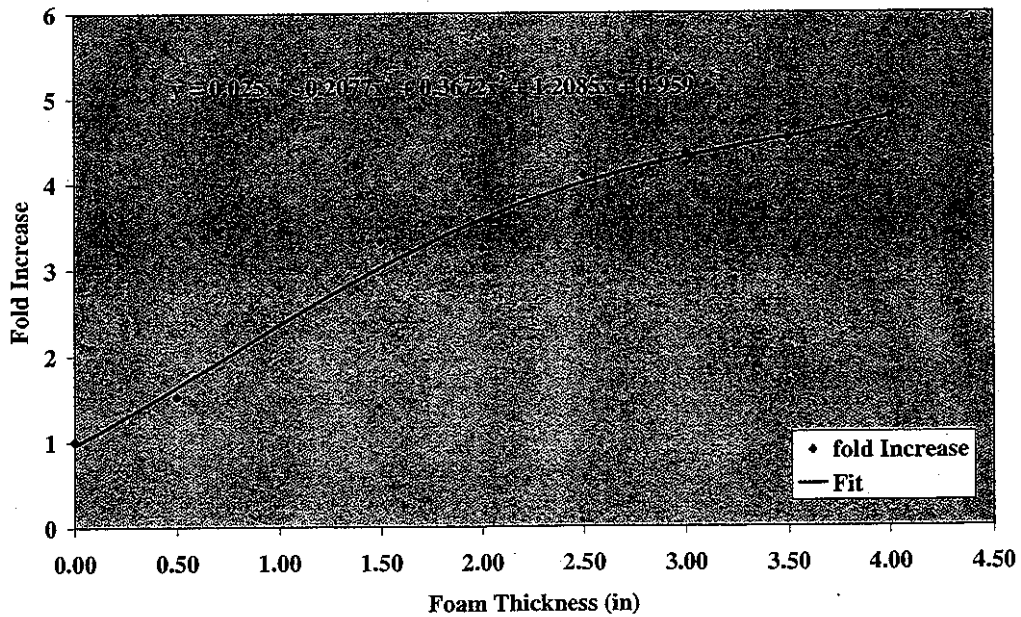


Figure 27: Crack fatigue life increase vs. Foam thickness (Cracked fuselage).

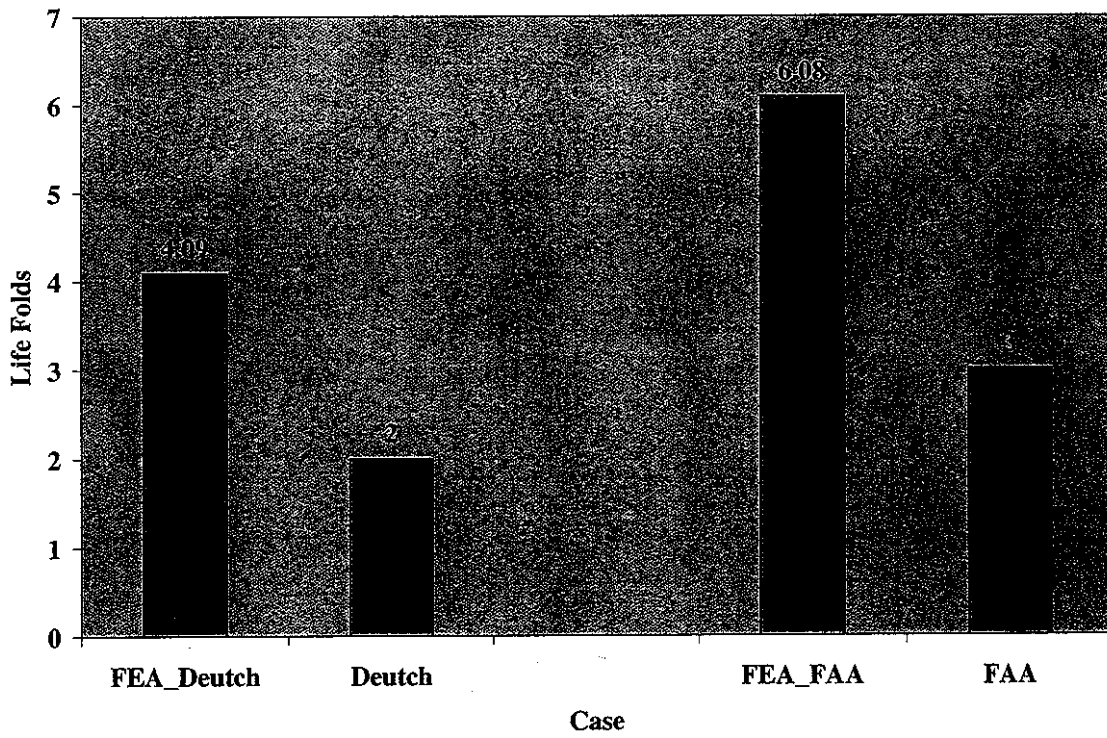


Figure 28: Effect of additional foam layer on crack growth life (Experimental results compared vs. FEA)